ACS Catalysis

Research Article

pubs.acs.org/acscatalysis

Noninnocent Nature of Carbon Support in Metal/Carbon Catalysts: Etching/Pitting vs Nanotube Growth under Microwave Irradiation

Evgeniy O. Pentsak, Evgeniy G. Gordeev, and Valentine P. Ananikov*

N. D. Zelinsky Institute of Organic Chemistry, Russian Academy of Sciences, Leninsky Prospect 47, 119991 Moscow, Russian Federation

Supporting Information

ABSTRACT: Microwave irradiation of Ni, Co, Cu, Ag, and Pt metal salts supported on graphite and charcoal revealed a series of carbon surface modification processes that varied depending on the conditions used (inert atmosphere, vacuum, or air) and the nature of metal salt. Carbon materials, routinely used to prepare supported metal catalysts and traditionally considered to be innocent on this stage, were found to actively change under the studied conditions: etching and pitting of the carbon surface by metal particles as well as growth of carbon nanotubes were experimentally observed by FE-SEM analysis. Catalyst preparation under microwave irradiation led to the formation of complex metal/carbon structures with significant changes in carbon morphology. These findings are of great value in developing an understanding of how M/C catalysts form and evolve and will help to design a new generation of efficient and stable catalysts. The energy surfaces of carbon support modification processes were studied with theoretical calculations at the density functional level. The energy surface of the multistage process of carbon nanotube formation from an etched graphene sheet was calculated for various types of carbon centers. These calculations indicated that interconversion of graphene layers and single wall carbon nanotubes is possible when cycloparaphenylene rings act as building units.

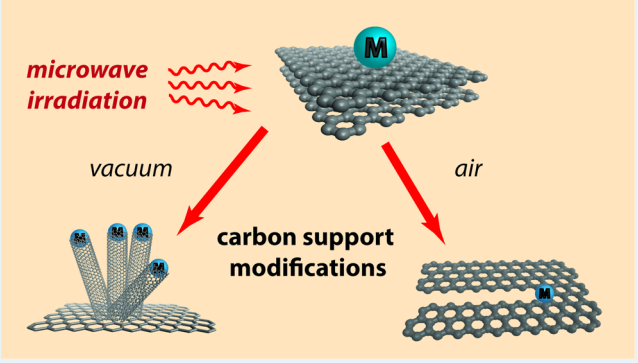

KEYWORDS: *metal nanoparticles, carbon support, microwave irradiation, M/C catalyst, carbon nanotubes, carbon pitting, carbon etching, semiempirical calculations*

1. INTRODUCTION

Carbon materials are utilized frequently as a support for metal clusters and metal nanoparticles in the preparation of metal on carbon (M/C) catalysts.[1] Microwave treatment is a well-established method for the preparation of M/C transition metal catalysts for industrial and laboratory applications.[2−4] The typical advantages of using carbon-supported catalysts include their high stability and the innocent nature of support as well as the ability to recycle such catalysts after use.[5] Variations in the preparation procedure used lead to supported catalysts with modulated activity at the metal centers.[6] Depending on the preparation method employed, metal particles may be weakly bound to the carbon surface or strongly bound to multiple carbon layers.

Metal/carbon catalysts have been successfully applied to mediate a number of important reactions in organic synthesis. Fascinating properties have been discovered for various Ni/C catalysts, for example, in cross-coupling, C−H and C−C bond formation, amination, hydrogenation, dehydrogenation, hydrodechlorination, carbonylation, and hydrothermal gasification reactions.[7] Other M/C catalysts have been found to be highly efficient for numerous transformations including C−H functionalization; formylation; Heck, Suzuki, and Sonogashira reactions; aromatization; H/D-labeling; hydrogenation; hydrodehalogenation; oxidation; dehydrogenation; and bio-oil processing.[8]

The field of carbon materials itself, stimulated by increasing interest in graphene systems, has grown tremendously in recent years.[9] Many different types of nanostructured carbon materials are accessible now with several promising areas of application in chemistry and catalysis.[10] Carbon materials have been modified using metal particles as catalysts, which successfully mediate the growth of various carbon nanostructures.[11] In a typical case, carbon-containing precursors (such as acetylene, ethylene, and methane) are passed over metal particles, leading to formation of carbon nanotubes. The hydrocarbon gas decomposes during contact with the molten metal particle, and dissolution of carbon into the metal takes place. Depending on the nature of metal−carbon interaction, a tip-growth model or base-growth model has been observed during formation of the nanotubes by this method.[12] Termination of the growth process occurs when carbon layers completely cover the surface of the metal particle, blocking further access of carbon precursor molecules to it.[13]

It should be emphasized that these two areas — the preparation of supported M/C catalysts and graphene research — are more or less studied independently of one another, although

Received: July 1, 2014
Revised: August 28, 2014
Published: September 11, 2014

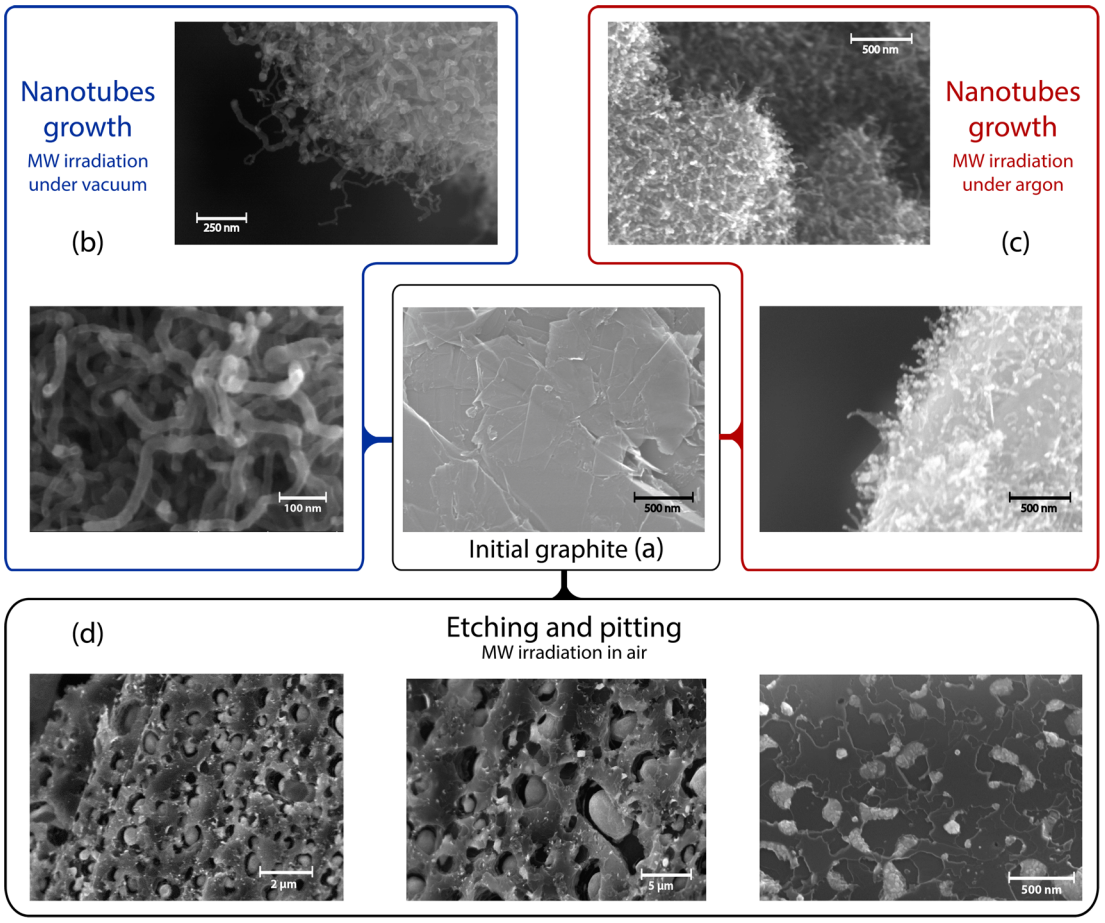

Figure 1. FE-SEM images of the studied Ni/C system: (a) - initial graphite system; (b) - after MW irradiation in vacuum conditions; (c) - after MW irradiation under Ar atmosphere; and (d) - after MW irradiation in air.

it is evident that interdisciplinary study of the two fields is extremely important for stimulating new developments and finding new areas of practical application.

In the present study, we investigated the behavior of the carbon support and the metal−carbon interactions that occur during M/C catalyst preparation under microwave irradiation (M = Ni, Co, Cu, Ag, and Pt). Several readily available metal salts were employed under regular conditions to prepare the M/C supported catalysts studied here. Nickel systems were of particular interest, as it has been shown that Ni may outperform more expansive Pd-based catalysts in several practical transformations.[14]

Surprisingly, we have found that catalyst preparation under routine conditions in certain cases initiates metal particle-mediated reactions that change the morphology of the carbon support. Preparation of the M/C catalysts involved mastering of the carbon surface with metal-mediated etching and carbon nanotube growth. The carbon support exhibited noninnocent behavior during the catalyst preparation stage.

2. RESULTS AND DISCUSSION

2.1. Modification of the Carbon Support during Ni/C Preparation. The morphology of the initial graphite surface is shown in Figure 1a. A uniform mixture of $Ni(acac)_2$ and graphite was prepared in two ways: 1) treatment of the solid mixture by ball milling and 2) impregnation of graphite by an aqueous solution of $Ni(acac)_2$ followed by solvent removal under reduced pressure. Both methods yielded a uniform distribution of $Ni(acac)_2$ on the graphite surface.

A homogenized solid mixture of $Ni(acac)_2$ and graphite was treated by directed adsorption of microwave radiation. Under an inert atmosphere of Ar or under vacuum conditions, the treatment resulted in the formation of plenty of carbon nanotubes with average diameters of 7−40 nm, lengths of 100−600 nm, and with the metal head located at the top position (Figures 1b and 1c). In sharp contrast, in the presence of oxygen, Ni particles formed patterns of pits and channels on their surface and penetrated inside the carbon material (Figure 1d). FE-SEM and EDX studies showed that microwave heating resulted in decomposition of $Ni(acac)_2$ via reduction by carbon, leading to metallic Ni particles with sizes around 5−50 nm and agglomerated particles up to 0.4 μm in size. The obtained metal particles possessed magnetic properties, which confirmed the formation of a metallic phase. It should be noted that the properties of agglomerated metal particles may substantially differ as compared to the initial state, thus having a noticeable impact on their catalytic effect.[5,15]

Apparently, the microwave irradiation created eddy currents on the surface of the formed nanoparticles,[16] which heated the particles, in a directed manner, to their melting temperature (also confirmed by observed nanoparticles agglomeration process). The melting process is also evident from the formation of pits and trenches in an oxidizing atmosphere. Numerous studies dealing with graphite dissolution into the molten metal particles were reported in the literature.[17] Thus, it is likely that the carbon

dx.doi.org/10.1021/cs500934g | ACS Catal. 2014, 4, 3806−3814

source for the growth of nanotubes in our experiment is a graphite support dissolved in the metal particle. After diffusion of carbon in the metal nanoparticles, further nanotubes growth apparently occurs according to the mechanism widely discussed in the literature.[12,13]

Based on a commonly accepted picture, it is possible that the observed nanotubes are formed by the dissolution of carbon in the metal particles, followed by a release of carbon after a concentration limit is reached within the particle.[13] This process may take place in an inert atmosphere (under Ar or vacuum).

In the oxygen-containing atmosphere, the released carbon was quickly oxidized to CO_2. Thus, molten nickel particles etched the surface of graphite to form trenches and recesses or penetrated it to form pores (Figure 1d). The reaction in air can be simply performed in an open reaction vessel. When the process was carried out under inert atmosphere or vacuum, the carbon released from the metal nanoparticles was not removed by oxidation and was therefore available to form a carbon nanotube. Nickel nanoparticles were located on the top of the nanotubes in the obtained material, indicating that a tip-growth mechanism was involved.

From a practical point of view, the process in vacuum is more convenient than in Ar because, in the latter case, heating generated a noticeable internal pressure inside the reaction vessel.

Our results are in good agreement with reports in the literature that microwave irradiation facilitates the formation of nanotubes from Fe particles.[18] Recently, experimental evidence of metal-mediated etching of graphene and HOPG was also reported.[19,17]

2.2. Theoretical Study of Graphene to Carbon Nanotube Transformation. The observed mastering of the carbon surface by metal particles is of particular importance, as it may facilitate the direct transformation of graphene layers into carbon nanotubes. This process may involve the initial formation of a hole in the graphene layer (due to etching), followed by nanotube growth directly on the top of the hole. Theoretical calculations were used to analyze the key aspect related to growth pathway and thermodynamics.

To estimate the thermodynamic parameters of direct graphene-to-nanotube conversion via an etching/growth mechanism, we carried out a computational study of a graphene sheet transformation into a model carbon nanotube with a diameter of 8.2 Å and (6,6) chirality (Figure 2a). Three different initial forms of graphene were studied: a layer completely capped with hydrogen atoms ($C_{408}H_{82}$), a partially capped layer ($C_{408}H_{58}$), and a pure carbon layer (C_{408}) as shown in Figure 2b.

Total energies were obtained by single point DFT calculations using the B3LYP, M06, M06L, and ωB97X-D potentials and the 6-31G(d) basis set (Figure 2d). Full geometry optimization of all structures was carried at the semiempirical PM6 level. Reliable accuracy of this computational procedure for the studies of carbon materials was confirmed previously.[20]

In the proposed model, the initial graphene sheet had a hole "burned" in it by a heated metal nanoparticle as observed under experimental conditions. The computational study showed that nanotube construction should be possible using [6]-cycloparaphenylene rings as building units (Figure 2a). Cycloparaphenylenes are the smallest cyclic segments enabling the armchair nanotube formation with (n,n) chirality.

First, we discuss the hydrogen-capped $C_{408}H_{82}$ model system (reaction (1); Figures 2c and 2d). For the model system, we assume that the process was accompanied by a release of hydrogen molecules upon the formation of carbon−carbon bonds during the nanotube growth.

A noticeable increase in the energy of the studied system was calculated for the beginning step as a result of the addition of the first cyclic segment to the edge of the hole (step I, Figure 2a). This energy change was caused by an increase in the strain upon the connection of a flat graphene sheet to a cylindrical tube (along with the energetically unfavorable cyclization process itself). Such a connection was provided by the formation of seven-membered cycles alternating with six-membered rings at the junction site of the tube and graphene sheet (Figure 2a and the Supporting Information).

In the next growth steps, the formation of structures II−VIII was accompanied by an approximately uniform increase in the energy; an increase of approximately 100 kcal/mol per one segment of the tube according to DFT calculations. Upon continued nanotube growth, a certain slowdown in the increase of the total energy of the system was calculated (steps VIII−X, Figure 2a). The overall calculated endothermic effect of the formation of nanotubes in this model was ∼1000 kcal/mol or 2.5 kcal/mol per one carbon atom.

To evaluate the performance of computational methods, several density functionals were compared. It should be noted that the results of the B3LYP, M06, M06L, and ωB97X-D calculations were in excellent agreement with each other (reaction (1), Figure 2d). Therefore, further calculations on reactions (2) and (3) were carried out using the ωB97X-D functional. It has been suggested that ωB97X-D may give a slightly better performance for graphene systems because it accounts for dispersion interactions.[21]

In the cases of $C_{408}H_{82}$ and $C_{408}H_{58}$ models hydrogen atoms at the armchair-edges (left and right edges of graphene sheet in Figure 2b) were moved at the new armchair-edges after formation of each new segment of nanotube. This allowed to minimize the energy changes due to the CH bonds dissociation and to analyze the energy changes due to the formation of new segments of the tube. Since several studies dedicated to the structure of graphene edges in a vacuum and under hydrogenation conditions have already been published,[22] the mechanism of the hydrogenation/dehydrogenation of graphene edges was not addressed in the present article.

Formation of the (6,6) nanotube from the partially hydrogen-capped $C_{408}H_{58}$ graphene sheet proceeded through similar structural evolution with a stepwise energy change. However, the overall reaction was highly exothermic and was accompanied by a decrease in total energy of −600 kcal/mol or −1.5 kcal/mol per one carbon atom (reaction (2); Figure 2d). The initial graphene sheet (Figure 2b), the overall transformation (Figure 2c), the energy surface (Figure 2d), and the structures for the stepwise transformation (Figures S12 and S13 in the Supporting Information) were elucidated for this process.

The exothermic effect was even more pronounced in the case of the pure carbon C_{408} layer (reaction (3); Figure 2d), where nanotube formation from the hydrogen-free graphene sheet was accompanied by an overall energy decrease of −1890 kcal/mol or −4.6 kcal/mol per one carbon atom.

The initial graphene sheet, the overall transformation, the energy surface (Figures 2b, 2c, and 2d, respectively), and the structures for the stepwise transformation (Figures S15 and S16 in the Supporting Information) were calculated for this process as well.

For comparison, relative energy changes of +2.5, −1.5, and −4.6 kcal/mol per carbon atom were calculated for reactions (1),

dx.doi.org/10.1021/cs500934g | ACS Catal. 2014, 4, 3806−3814

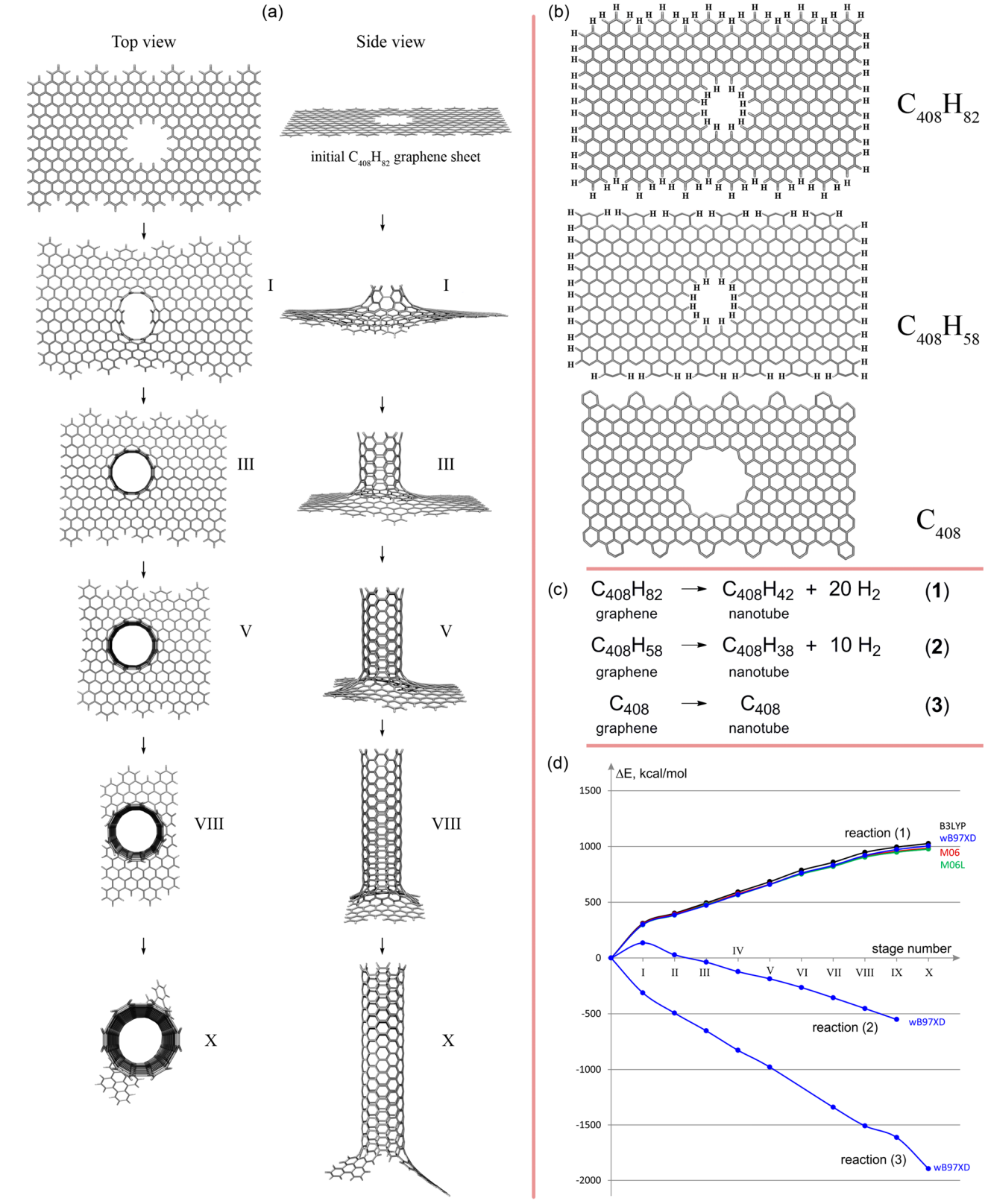

Figure 2. (a) - Calculated structures in the stepwise transformation of a $C_{408}H_{82}$ graphene sheet to a (6,6) nanotube (selected structures are shown, see the Supporting Information for complete details); (b) - molecular structures of the initial $C_{408}H_{82}$, $C_{408}H_{58}$, and C_{408} graphene sheets; (c) - overall nanotube formation reactions for the $C_{408}H_{82}$, $C_{408}H_{58}$, and C_{408} graphene sheets; (d) - relative energies of reactions (1−3) calculated at the specified DFT levels.

(2), and (3), respectively (Figure 2). The origin of these drastic energy changes becomes clear if we calculate the relative stability of the initial graphene sheets (Figure 2b): 0, 2000, and 5200 kcal/mol for the $C_{408}H_{82}$, $C_{408}H_{58} + 12H_2$, and $C_{408} + 41H_2$ systems, respectively. Thus, upon removal of its hydrogen caps, the graphene layer becomes destabilized due to the introduction

dx.doi.org/10.1021/cs500934g | ACS Catal. 2014, 4, 3806−3814

of carbon atoms with unsaturated valency located at its edges. Formation of carbon−carbon bonds during nanotube growth gradually decreases the overall energy of the system and renders the process exothermic. Note that in Figure 2d, all of the reactions are shown as separate energy trends relative to their respective initial graphene layers that were set to 0 kcal/mol. An overall energy diagram with a common zero point was also calculated and showed trends similar to those discussed above (Figure S18, Supporting Information).

As shown in Figure 2d, the formation of nanotube is energetically favorable for the $C_{408}H_{58}$ and C_{408} graphene sheets, that is, for the sheets containing noncapped carbon atoms at the edges. Thus, a possible driving force of the process in these cases is related to energy gain due to decreasing the number of edge carbon atoms and their binding to each other.

Thus, the chemical nature of the graphene edge is the key parameter affecting the feasibility of the studied nanotube growth process. The thermodynamic factor of nanotube formation from a graphene sheet is strongly dependent on the state of the edge of sheet, where nanotube formation from a nonhydrogenated graphene sheet was found to be an energetically favorable process, while capping the carbon perimeter decreased the exothermic effect.

It should be noted that such nanotube formation may take place in the oxygen-free environment under vacuum or in an Ar atmosphere, where etching by metal particles produces uncapped carbon edges (in agreement with experiment). In the presence of oxygen, carbon atoms on the edges were capped by the formation of C═O groups, which prevented formation of the nanotube and directed the process to etching/pitting and elimination of CO_2.

2.3. Side Processes during M/C Preparation. Metal particles are expected to be bound to the surface of the carbon support or more strongly bound to multiple carbon layers in typical prepared M/C catalysts (Figures 3a and b). These are the main processes taking place during supported catalyst preparation.

Indeed, our FE-SEM study of the Ni/C supported catalyst, prepared under microwave irradiation, showed that the carbon support was not inert and did not remain intact during the treatment. Two types of side processes may take place during catalyst preparation: (i) formation of pits or channels on the surface and penetration of metal particles into the carbon material in the presence of oxidizer (Figures 3c and d) and (ii) nanotube growth in an oxygen-free atmosphere (Figures 3e and f). To the best of our knowledge, such evolution of the carbon support during catalyst preparation has not yet been considered in detail.

Upon investigation, it was also found that the type of the metal salt plays an important role in M/C system formation. When $NiCl_2$ rather than $Ni(acac)_2$ was employed as the precursor under vacuum or in Ar, carbon nanostructure formation was not observed (conditions similar to those used for Figures 1b and 1c), but doing so did cause pits and channels to form in the presence of air (under conditions similar to those used for Figure 1d).

The results prompted us to study possible transformations of the carbon support upon microwave treatment of M/C systems made with different metal salts, as summarized in Table 1. All studied systems showed noticeable modifications of the carbon surface upon microwave irradiation in air. Indeed, pitting/etching type modifications were observed for the Ni, Co, Cu, Ag, and Pt salts studied (Table 1). This finding suggests that the appearance of heated metal particles on the carbon surface gradually facilitates the process.

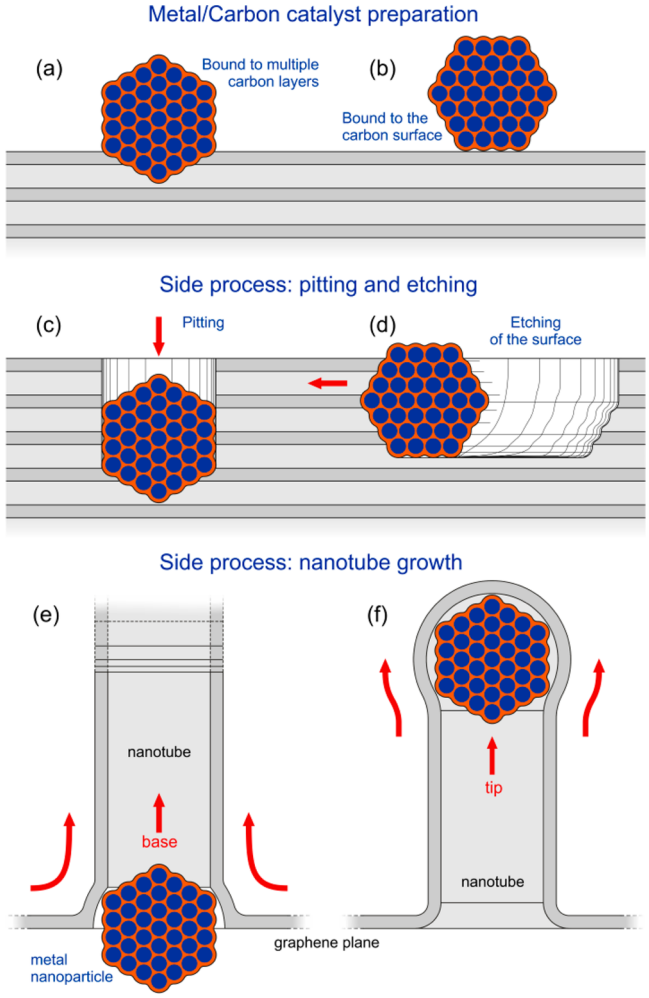

Figure 3. (a, b) − Deposition of a metal particle on the surface to prepare a supported catalyst; (c, d) − burning channels and etching the surface of carbon materials; (e, f) − base-growth and tip-growth mechanisms for metal-mediated carbon nanotube formation.

Table 1. Transformations of Carbon Support upon Microwave Irradiation in the Presence of Supported Metal Particles[a]

entry	metal salt	pitting/etching (in air)	CNT growth (under vacuum)
1	$Ni(acac)_2$	+	+
2	$Ni(OAc)_2$	+	+
3	$NiCl_2$	+	-
4	$Co(acac)_2$	+	+
5	$CoCl_2$	+	-
6	$Cu(acac)_2$	+	-
7	$Cu(OAc)_2$	+	-
8	$AgNO_3$	+	-
9	$PtCl_4$	+	-

[a]Pitting/etching under vacuum was not observed for the studied systems.

Both pitting/etching in air and carbon nanotube growth under vacuum were observed for $Ni(acac)_2$, $Ni(OAc)_2$, and $Co(acac)_2$ metal precursors (entries 1, 2, 4; Table 1). In the case of the experimental Ni/C system studied here, the tip-growth model was predominant (Figure 3f and Figures 1b,c). In contrast, $NiCl_2$ and $CoCl_2$ did not mediate carbon nanotube growth. Neither of the studied Cu, Ag, and Pt salts resulted in the nanotube

dx.doi.org/10.1021/cs500934g | ACS Catal. 2014, 4, 3806−3814

formation. Thus, pitting/etching is a general process for the M/C systems, whereas nanotube growth is more specific and may be expected in a fewer number of cases.

Under both types of conditions—in air and under vacuum—the degree of carbon surface modification was dependent on the irradiation time. Decreasing microwave treatment time to <1 min produced modifications at the trace level, whereas an irradiation time of 15 min led to noticeable modifications of the carbon support.

It should be pointed out that when heated by MW irradiation under vacuum conditions, several metal salts, including $NiCl_2$, $CoCl_2$, $Cu(acac)_2$, $Cu(OAc)_2$, $AgNO_3$, and $PtCl_4$ (entries 3, 5–9; Table 1), did not observably change the carbon support. Neither pitting/etching nor nanotube growth were detected.

One of the key factors for the nanotube formation is the absence of an oxidizing atmosphere. It is also obvious that the nature of the metal affected growth of the nanotubes. We observed the growth of nanotubes with nickel acetylacetonate and nickel acetate, whereas the nanotubes growth did not occur with the same copper salts. This may be due to the high affinity of Co and Ni to carbon as compared with Cu and Ag[23,12c] and also due to the high solubility of carbon in these metals.[24] Another important factor concerns the size of the metal particles, since nanotubes growth did not occur on metal particles with the size larger than 50 nm.

The nature of the metal salt also plays an important role in the nanotube formation process. Reduction of the metal chlorides is more difficult in comparison with the reduction of the acetates and acetylacetonates. Most likely, it is a reason for the lack of growth of nanotubes in the case Ni and Co chlorides.

To test the effect of the nature of the carbon material on the growth of nanotubes, we carried out the experiments using charcoal instead of graphite. In this case we have also observed the formation of carbon nanotubes.

Pitting and etching processes are less sensitive to the metal precursors and took place regardless of the metal source used. It should be noted that the etching process occurred preferentially on smooth surfaces of graphite sheets, where the metal particle is free to slide along the graphene surface. On the contrary, pitting process occurred more frequently on the defective surface, such as on the side surfaces of graphite formed by the edges of graphene sheets. The pitting process was also observed using other carbon materials with porous structure such as charcoal. Concerning the particles sizes, pitting was more typical for larger metal particles, while etching was frequently observed for smaller metal particles.

3. CONCLUSIONS

In summary, the often-assumed inert nature of carbon supports cannot be taken for granted for all M/C catalysts. A variety of side processes (nanotube growth, pitting, and etching) may take place during the catalyst preparation depending on the conditions used. The degree of carbon support modification can be reduced by carrying out the catalyst preparation under vacuum and by selecting an appropriate metal salt.

The present study has shown a strong correlation between the processes taking place during the growth of ordered carbon structures (graphene and nanotubes) and the processes involved in the formation of metal catalysts on the carbon support. Thus, it was important to consider the possibility of direct conversion of graphene layers to a carbon nanotube via metal-mediated etching and sequential attachment of cycloparaphenylene rings. The theoretical estimation at the DFT level that was carried out in the present study showed that, for an uncapped or partially capped graphene layer, this process is feasible from a thermodynamic point of view.

We anticipate that modification of the carbon support may take place not only during catalyst preparation, as discussed in this study, but also during the operation of metal/carbon catalysts in the reactions. These processes may have a dramatic effect on catalyst activity and stability, and, as such, the topic will be further addressed in our ongoing research.

The aim of the present study was to address the noninnocent nature of the carbon support and to describe possible transformations of the M/C catalysts. An interesting opportunity would be to use the observed side-reactions in order to modify the catalyst and promote new catalytic activity. The present study revealed a possibility to place metal particles inside the pits and channels of the carbon support. This may help to stabilize the catalyst particles and to form a kind of nanoreactors inside the carbon materials (Figure 3). Important to point out, that the catalyst particles as well as the channels and pits were made simply by applying microwave irradiation. A challenging point in this regard is to achieve the arrangement of uniform nanostructures with a narrow particle size distribution.

4. EXPERIMENTAL PROCEDURE

4.1. General Methods and Materials. Commercial $Ni(acac)_2$ (Sigma-Aldrich; CAS number 3264-82-2) was dried in vacuum before use (0.95 mbar, 80 °C, 2 h). The surface of the carbon material used was represented with ensembles of graphene layers within the structure of graphite (FE-SEM characterization).

Microwave treatment was carried out using a Panasonic 2M210-M1 magnetron operating at a frequency of 2455 MHz. For the homogenization of reaction mixtures, a ball mill treatment was used (stainless steel reactor with two stainless balls; ball diameter 10 mm, ball weight 4 g, reactor diameter 28 mm, frequency 50 Hz).

FE-SEM measurements were performed using a Hitachi SU8000 microscope. For FE-SEM measurements, the samples were mounted on a 25 mm aluminum specimen stub and fixed with a conductive silver paint. The FE-SEM images were processed (the average diameter and length of carbon nanotubes and sizes of graphite modifications were measured) using the Image Tool software package.

Unless noted otherwise, experiments were conducted in quartz round-bottom flasks.

4.2. Homogenization of Metal Salt/Carbon Material Mixture. Ball milling: dried powders of graphite (50 mg) and nickel salt (10 mg) were placed into the ball mill and treated for 90 min.

Impregnation: nickel salt (10 mg) was dissolved in water (8 mL), followed by the addition of 50 mg of graphite. Dissolution and stirring were promoted by sonication (10 min). After formation of uniform suspension, water was removed under reduced pressure.

Similar procedures were applied for the other metal precursors.

4.3. Typical M/C Preparation Procedure. A mixture of $Ni(acac)_2$ (10 mg) and graphite (50 mg) was placed into a quartz round-bottom flask after homogenization. The flask remained open for experiments performed under air. For vacuum conditions, the flask was sealed by silicone septum and evacuated to 0.5 mbar. For Ar conditions, the flask was purged with Ar for 5 min and then was sealed with a silicone septum. The reaction mixture was treated by microwave irradiation for 5 to 30 min.

dx.doi.org/10.1021/cs500934g | ACS Catal. 2014, 4, 3806–3814

A similar procedure was applied for the other metal precursors and other carbon materials.

4.4. Theoretical Calculations. B3LYP,[25] M06,[26] M06L,[27] and ωB97X-D[28] calculations were performed with the 6-31G(d) basis set.[29] All DFT calculations were performed using the Gaussian 09[30] program package. A single point energy evaluation was carried out for structures fully optimized by the PM6[31] semiempirical method implemented in the MOPAC 2012 program.[32]

To evaluate the performance of the utilized theory level, calculations were carried out on the known transformation of a plane C_{117} graphene sheet to C_{60} fullerene. At the B3LYP/6-31G(d)//PM6 theory level (full optimization by the PM6 method and a subsequent single point total energy calculation at the B3LYP/6-31G(d) level), the transformation was characterized by an energy change of 0.268 eV/atom, while the value reported in the literature was 0.261 eV/atom.[33] Thus, the geometrical parameters obtained by the PM6 method were considered reliable for the evaluation of the total energy of carbon nanostructures by density functional methods. An extensive evaluation of the accuracy of DFT//PM6 calculations for carbon materials was also reported earlier for other systems.[20]

■ ASSOCIATED CONTENT

Supporting Information

(i) FE-SEM images of modified carbon surface; (ii) optimized molecular structures for $C_{408}H_{82}$, $C_{408}H_{58}$, and C_{408} graphene sheets at the PM6 level for each stage of the (6,6) nanotube growth process; (iii) tables and plots containing full energy trends of all stages of the nanotube growth process at B3LYP, M06, M06-L, ωB97X-D (for $C_{408}H_{82}$ graphene sheet), and ωB97X-D (for $C_{408}H_{58}$ and C_{408} graphene sheets). This material is available free of charge via the Internet at http://pubs.acs.org.

■ AUTHOR INFORMATION

Corresponding Author

*E-mail: val@ioc.ac.ru.

Notes

The authors declare no competing financial interest.

■ ACKNOWLEDGMENTS

The authors are grateful to Dr. Kseniya S. Egorova for helpful discussions. Financial support of the Russian Science Foundation is acknowledged (RNF Grant 14-13-01030). Usage of computational resources of the Supercomputing Center of Lomonosov Moscow State University is acknowledged.

■ REFERENCES

(1) (a) White, R. J.; Luque, R.; Budarin, V. L.; Clark, J. H.; Macquarrie, D. J. *Chem. Soc. Rev.* **2009**, *38*, 481−494. (b) Wildgoose, G. G.; Banks, C. E.; Compton, R. G. *Small* **2006**, *2*, 182−193. (c) Xu, C.; Wang, X.; Zhu, J. *J. Phys. Chem. C* **2008**, *112*, 19841−19845. (d) Georgakilas, V.; Gournis, D.; Tzitzios, V.; Pasquato, L.; Guldi, D. M.; Prato, M. *J. Mater. Chem.* **2007**, *17*, 2679−2694.

(2) (a) Serp, P. Carbon nanotubes and nanofibers in catalysis. In *Carbon Materials for Catalysis*; Serp, P., Figueiredo, J. L., Eds.; John Wiley & Sons, Inc.: Hoboken, NJ, 2009; pp 309−372. (b) Scheuermann, G. M.; Rumi, L.; Steurer, P.; Bannwarth, W.; Mülhaupt, R. *J. Am. Chem. Soc.* **2009**, *131*, 8262−8270. (c) De Jong, K. P.; Geus, J. W. *Catal. Rev.* **2000**, *42*, 481−510. (d) Ananikov, V. P.; Khemchyan, L. L.; Ivanova, Yu. V.; Bukhtiyarov, V. I.; Sorokin, A. M.; Prosvirin, I. P.; Vatsadze, S. Z.; Medved'ko, A. V.; Nuriev, V. N.; Dilman, A. D.; Levin, V. V.; Koptyug, I. V.; Kovtunov, K. V.; Zhivonitko, V. V.; Likholobov, V. A.; Romanenko, A. V.; Simonov, P. A.; Nenajdenko, V. G.; Shmatova, O. I.; Muzalevskiy, V. M.; Nechaev, M. S.; Asachenko, A. F.; Morozov, O. S.; Dzhevakov, P. B.; Osipov, S. N.; Vorobyeva, D. V.; Topchiy, M. A.; Zotova, M. A.; Ponomarenko, S. A.; Borshchev, O. V.; Luponosov, Y. N.; Rempel, A. A.; Valeeva, A. A.; Stakheev, A. Yu.; Turova, O. V.; Mashkovsky, I. S.; Sysolyatin, S. V.; Malykhin, V. V.; Bukhtiyarova, G. A.; Terent'ev, A. O.; Krylov, I. B. *Russ.Chem.Rev.* **2014**, *83*, 885−985. (e) Auer, E.; Freund, A.; Pietsch, J.; Tacke, T. *Appl. Catal., A* **1998**, *173*, 259−271. (f) Vairavapandian, D.; Vichchulada, P.; Lay, M. D. *Anal. Chim. Acta* **2008**, *626*, 119−129.

(3) (a) Kharissova, O. V.; Zavala, E.; Ortíz, U.; Hernández-Piñero, J. L.; Soloviev, S. *MRS Proc.* **2011**, *821*, 3.19. (b) Varadan, V. K.; Hollinger, R. D.; Varadan, V. V.; Xie, J.; Sharma, P. K. *Smart Mater. Struct.* **2000**, *9*, 413−420. (c) Choi, Y. C.; Bae, D. J.; Lee, Y. H.; Lee, B. S.; Han, I. T.; Choi, W. B.; Lee, N. S.; Kim, J. M. *Synth. Met.* **2000**, *108*, 159−163. (d) Zhang, X.; Liu, Z. *Nanoscale* **2012**, *4*, 707−714. (e) Hong, E. H.; Lee, K. H.; Oh, S. H.; Park, C. G. *Adv. Funct. Mater.* **2003**, *13*, 961−966. (f) Zhang, X.; Manohar, S. K. *Chem. Commun.* **2006**, 2477−2479. (g) Yuan, G. D.; Zhang, W. J.; Yang, Y.; Tang, Y. B.; Li, Y. Q.; Wang, J. X.; Meng, X. M.; He, Z. B.; Wu, C. M. L.; Bello, I.; Lee, C. S.; Lee, S. T. *Chem. Phys. Lett.* **2009**, *467*, 361−364. (h) Varadan, V. K.; Xie, J. *Smart Mater. Struct.* **2002**, *11*, 728−734. (i) Marcinek, M.; Song, X.; Kostecki, R. *Electrochem. Commun.* **2007**, *9*, 1739−1743. (j) Kim, U.; Pcionek, R.; Aslam, D. M.; Tománek, D. *Diamond Relat. Mater.* **2001**, *10*, 1947−1951. (k) Wang, G.; Zhang, Q.; Yoon, S. F.; Ahn, J. *Scr. Mater.* **2003**, *48*, 409−412. (l) Bo, Z.; Yang, Y.; Chen, J.; Yu, K.; Yan, J.; Cen, K. *Nanoscale* **2013**, *5*, 5180−5204.

(4) (a) Siamaki, A. R.; Khder, A. E. R. S.; Abdelsayed, V.; El-Shall, M. S.; Gupton, B. F. *J. Catal.* **2011**, *279*, 1−11. (b) Tian, Z. Q.; Jiang, S. P.; Liang, Y. M.; Shen, P. K. *J. Phys. Chem. B* **2006**, *110*, 5343−5350. (c) Marquardt, D.; Vollmer, C.; Thomann, R.; Steurer, P.; Mülhaupt, R.; Redel, E.; Janiak, C. *Carbon* **2011**, *49*, 1326−1332. (d) Boxall, D. L.; Lukehart, C. M. *Chem. Mater.* **2001**, *13*, 806−810. (e) Motshekga, S. C.; Pillai, S. K.; Sinha Ray, S. S.; Jalama, K.; Krause, R. W. M. *J. Nanomater.* **2012**, *2012*, 691503.

(5) (a) Rodríguez-Reinoso, F. *Carbon* **1998**, *36*, 159−175. (b) Serp, P.; Corrias, M.; Kalck, P. *Appl. Catal., A* **2003**, *253*, 337−358. (c) Serp, P.; Castillejos, E. *ChemCatChem* **2010**, *2*, 41−47.

(6) (a) Zhu, J.; Holmen, A.; Chen, D. *ChemCatChem* **2013**, *5*, 378−401. (b) Solhy, A.; Machado, B. F.; Beausoleil, J.; Kihn, Y.; Gonçalves, F.; Pereira, M. F. R.; Órfão, J. J. M.; Figueiredo, J. L.; Faria, J. L.; Serp, P. *Carbon* **2008**, *46*, 1194−1207.

(7) (a) An, C.; Liu, G.; Li, L.; Wang, Y.; Chen, C.; Wang, Y.; Jiao, L.; Yuan, H. *Nanoscale* **2014**, *6*, 3223−3230. (b) Galindo-Hernández, F.; Wang, J.-A.; Chen, L.; Bokhimi, X.; Pérez-Larios, A.; Gómez, R. *J. Mater. Res.* **2013**, *28*, 3297−3309. (c) Peng, T.; Zhang, X.; Zeng, P.; Li, K.; Zhang, X.; Li, X. *J. Catal.* **2013**, *303*, 156−163. (d) Wang, Y.; Wang, J.; Fan, G.; Li, F. *Catal. Commun.* **2012**, *19*, 56−60. (e) Lipshutz, B. H.; Blomgren, P. A. *J. Am. Chem. Soc.* **1999**, *121*, 5819−5820. (f) Lipshutz, B. H.; Butler, T.; Swift, E. *Org. Lett.* **2008**, *10*, 697−700. (g) Butler, T. A.; Swift, E. C.; Lipshutz, B. H. *Org. Biomol. Chem.* **2008**, *6*, 19−25. (h) Lipshutz, B. H.; Frieman, B. A.; Lee, C. T.; Lower, A.; Nihan, D. M.; Taft, B. R. *Asian J. Chem.* **2006**, *1*, 417−429. (i) Zeng, P.; Zhang, X.; Zhang, X.; Chai, B.; Peng, T. *Chem. Phys. Lett.* **2011**, *503*, 262−265. (j) Luo, J.; Li, J.; Shen, D.; He, L.; Tong, D.; Hy, C. *Sci. China Chem.* **2010**, *53*, 1487−1491. (k) Zhang, Q.; Wang, H. F.; Sun, G. S.; Huang, K. L.; Fang, W. P.; Yang, Y. Q. *Chin. J. Catal.* **2009**, *30*, 555−559. (l) Zhang, Q.; Wang, H. F.; Sun, G. S.; Huang, K. L.; Fang, W. P.; Yang, Y. Q. *J. Nat. Gas Chem.* **2008**, *17*, 355−358. (m) Srebowata, A.; Stefanowicz-Pieta, I.; Juszczyk, W.; Karpinski, Z. *Polish J. Chem.* **2007**, *81*, 1521−1529. (n) Sharma, A.; Saito, I.; Nakagawa, H.; Miura, K. *Fuel* **2007**, *86*, 915−920. (o) Lipshutz, B. H.; Frieman, B. A.; Butler, T.; Kogan, V. *Angew. Chem., Int. Ed.* **2006**, *45*, 800−803. (p) Frieman, B. A.; Taft, B. R.; Lee, C.-T.; Butler, T.; Lipshutz, B. H. *Synthesis* **2005**, 2989−2993.

(8) (a) Chinchilla, R.; Najera, C. *Chem. Rev.* **2014**, *114*, 1783−1826. (b) Tang, D.-T. D.; Collins, K. D.; Ernst, J. B.; Glorius, F. *Angew. Chem., Int. Ed.* **2014**, *53*, 1809−1813. (c) Taladriz-Blanco, P.; Hervés, P.; Pérez-Juste, J. *Top. Catal.* **2013**, *56*, 1154−1170. (d) Yu, B.; Zhao, Y.; Zhang, H.; Xu, J.; Hao, L.; Gao, X.; Liu, Z. *Chem. Commun.* **2014**, *50*, 2330−2333. (e) Agostini, G.; Lamberti, C.; Pellegrini, R.; Leofanti, G.;

Giannici, F.; Longo, A.; Groppo, E. *ACS Catal.* **2014**, *4*, 187−194. (f) Kurokhtina, A. A.; Larina, E. V.; Schmidt, A. F.; Malaika, A.; Krzyżyńska, B.; Rechnia, P.; Kozłowski, M. *J. Mol. Catal. A: Chem.* **2013**, *379*, 327−332. (g) Gunawan, R.; Li, X.; Lievens, C.; Gholizadeh, M.; Chaiwat, W.; Hu, X.; Mourant, D.; Bromly, J.; Li, C.-Z. *Fuel* **2013**, *111*, 709−717. (h) Sugiyama, S.; Tanaka, H.; Bando, T.; Nakagawa, K.; Sotowa, K.-I.; Katou, Y.; Mori, T.; Yasukawa, T.; Ninomiya, W. *Catal. Today* **2013**, *203*, 116−121. (i) Yin, M.; Natelson, R. H.; Campos, A. A.; Kolar, P.; Roberts, W. L. *Fuel* **2013**, *103*, 408−413. (j) Maegawa, T.; Kitamura, Y.; Sako, S.; Udzu, T.; Sakurai, A.; Tanaka, A.; Kobayashi, Y.; Endo, K.; Bora, U.; Kurita, T.; Kozaki, A.; Monguchi, Y.; Sajiki, H. *Chem.—Eur. J.* **2007**, *13*, 5937−5943. (k) Gadge, S. T.; Bhanage, B. M. *J. Org. Chem.* **2013**, *78*, 6793−6797. (l) Wang, Y.; Yao, J.; Li, H.; Su, D.; Antonietti, M. *J. Am. Chem. Soc.* **2011**, *133*, 2362−2365. (m) Tarasov, A. L.; Kirichenko, O. A.; Tolkachev, N. N.; Mishin, I. V.; Kalenchuk, A. N.; Bogdan, V. I.; Kustov, L. M. *Russ. J. Phys. Chem. A* **2010**, *84*, 1122−1126. (n) Kurita, T.; Aoki, F.; Mizumoto, T.; Maejima, T.; Esaki, H.; Maegawa, T.; Monguchi, Y.; Sajiki, H. *Chem.—Eur. J.* **2008**, *14*, 3371−3379. (o) Nakamichi, N.; Kawashita, Y.; Hayashi, M. *Org. Lett.* **2002**, *4*, 3955−3957. (p) Heidenreich, R. G.; Kohler, K.; Krauter, J. G. E.; Pietsch, J. *Synlett* **2002**, 1118−1122. (q) Felpin, F.-X.; Ayad, T.; Mitra, S. *Eur. J. Org. Chem.* **2006**, 2679−2690. (r) Seki, M. *Synthesis* **2006**, 2975−2992. (s) Sakurai, H.; Tsukuda, T.; Hirao, T. *J. Org. Chem.* **2002**, *67*, 2721−2722. (t) Gómez-Sainero, M.; Seoane, X. L.; Fierro, J. L. G.; Arcoya, A. *J. Catal.* **2002**, *209*, 279−288.

(9) (a) Geim, A. K.; Novoselov, K. S. *Nat. Mater.* **2007**, *6*, 183−191. (b) Rao, C. N. R.; Sood, A. K.; Subrahmanyam, K. S.; Govindaraj, A. *Angew. Chem., Int. Ed.* **2009**, *48*, 7752−7777. (c) Stankovich, S.; Dikin, D. A.; Dommett, G. H. B.; Kohlhaas, K. M.; Zimney, E. J.; Stach, E. A.; Piner, R. D.; Nguyen, S. T.; Ruoff, R. S. *Nature* **2006**, *442*, 282−286. (d) Park, S.; Ruoff, R. S. *Nat. Nanotechnol.* **2009**, *4*, 217−224. (e) Allen, M. J.; Tung, V. C.; Kaner, R. B. *Chem. Rev.* **2010**, *110*, 132−145. (f) James, D. K.; Tour, J. M. *Acc. Chem. Res.* **2013**, *46*, 2307−2318. (g) Huang, J.; Liu, Y.; You, T. *Anal. Methods* **2010**, *2*, 202−211.

(10) (a) Machado, B. F.; Serp, P. *Catal. Sci. Technol.* **2012**, *2*, 54−75. (b) Bitter, J. H. *J. Mater. Chem.* **2010**, *20*, 7312−7321. (c) Ledoux, J.; Vieira, R.; Pham-Huu, C.; Keller, N. *J. Catal.* **2003**, *216*, 333−342. (d) Yang, L.; Zhao, Y.; Chen, S.; Wu, Q.; Wang, X.; Hu, Z. *Chin. J. Catal.* **2013**, *34*, 1986−1991. (e) Konwar, L. J.; Boro, J.; Deka, D. *Renewable Sustainable Energy Rev.* **2014**, *29*, 546−564. (f) Wang, D.-W.; Su, D. *Energy Environ. Sci.* **2014**, *7*, 576−591. (g) Yang, Z.; Nie, H.; Chen, X.; Chen, X.; Huang, S. *J. Power Sources* **2013**, *236*, 238−249.

(11) (a) Esconjauregui, S.; Whelan, C. M.; Maex, K. *Carbon* **2009**, *47*, 659−669. (b) Inami, N.; Mohamed, M. A.; Shikoh, E.; Fujiwara, A. *Sci. Technol. Adv. Mater.* **2007**, *8*, 292−295. (c) Ding, F.; Larsson, P.; Larsson, J. A.; Ahuja, R.; Duan, H.; Rosén, A.; Bolton, K. *Nano Lett.* **2008**, *8*, 463−468. (d) Bult, J. B.; Sawyer, W. G.; Ajayan, P. M.; Schadler, L. S. *Nanotechnol.* **2009**, *20*, 085302. (e) Jourdain, V.; Bichara, C. *Carbon* **2013**, *58*, 2−39. (f) Yamada, T.; Namai, T.; Hata, K.; Futaba, D. N.; Mizuno, K.; Fan, J.; Yudasaka, M.; Yumura, M.; Iijima, S. *Nat. Nanotechnol.* **2006**, *1*, 131−136. (g) Willems, I.; Kónya, Z.; Colomer, J. F.; Van Tendeloo, G.; Nagaraju, N.; Fonseca, A.; Nagy, J. B. *Chem. Phys. Lett.* **2000**, *317*, 71−76.

(12) (a) Tessonnier, J. P.; Su, D. S. *ChemSusChem* **2011**, *4*, 824−847. (b) Gavillet, J.; Loiseau, A.; Ducastelle, F.; Thair, S.; Bernier, P.; Stéphan, O.; Thibault, J.; Charlier, J. C. *Carbon* **2002**, *40*, 1649−1663. (c) Raty, J. Y.; Gygi, F.; Galli, G. *Phys. Rev. Lett.* **2005**, *95*, 096103. (d) Kumar, M.; Ando, Y. *J. Nanosci. Nanotechnol.* **2010**, *10*, 3739−3758. (e) Gohier, A.; Ewels, C. P.; Minea, T. M.; Djouadi, M. A. *Carbon* **2008**, *46*, 1331−1338. (f) Deng, W.-Q.; Xu, X.; Goddard, W. A. *Nano Lett.* **2004**, *4*, 2331−2335.

(13) Kumar, M. Carbon Nanotube Synthesis and Growth Mechanism. In *Carbon Nanotubes - Synthesis, Characterization, Applications*; Yellampalli, S., Eds.; InTech: 2011.

(14) (a) Beletskaya, I. P.; Ananikov, V. P. *Chem. Rev.* **2011**, *111*, 1596−1636. (b) Ananikov, V. P.; Beletskaya, I. P. *Dalton Trans.* **2011**, *40*, 4011−4023. (c) Zheng, J.; Roisnel, T.; Darcel, C.; Sortais, J.-B. *ChemCatChem* **2013**, *5*, 2861−2864. (d) LaGrow, A. P.; Ingham, B.; Toney, M. F.; Tilley, R. D. *J. Phys. Chem. C* **2013**, *117*, 16709−16718. (e) Ganushevich, Y. S.; Miluykov, V. A.; Polyancev, F. M.; Latypov, S. K.; Lönnecke, P.; Hey-Hawkins, E.; Yakhvarov, D. G.; Sinyashin, O. G. *Organometallics* **2013**, *32*, 3914−3919. (f) Li, J.; Huang, H.; Liang, W.; Gao, Q.; Duan, Z. *Org. Lett.* **2013**, *15*, 282−285. (g) Sui, A.; Shi, X.; Wu, S.; Tian, H.; Geng, Y.; Wang, F. *Macromolecules* **2012**, *45*, 5436−5443. (h) Ananikov, V. P.; Gayduk, K. A.; Starikova, Z. A.; Beletskaya, I. P. *Organometallics* **2010**, *29*, 5098−5102. (i) Zheng, J.; Darcel, C.; Sortais, J.-B. *Catal. Sci. Technol.* **2013**, *3*, 81−84. (j) Beaver, M. G.; Jamison, T. F. *Org. Lett.* **2011**, *13*, 4140−4143. (k) Zhang, X.; Liu, H.; Hu, X.; Tang, G.; Zhu, J.; Zhao, Y. *Org. Lett.* **2011**, *13*, 3478−3481. (l) Wu, L.; Ling, J.; Wu, Z.-Q. *Adv. Synth. Catal.* **2011**, *353*, 1452−1456. (m) Ananikov, V. P.; Orlov, N. V.; Kabeshov, M. A.; Beletskaya, I. P.; Starikova, Z. A. *Organometallics* **2008**, *27*, 4056−4061.

(15) O'Byrne, J. P.; Li, Z.; Jones, S. L. T.; Fleming, P. G.; Larsson, J. A.; Morris, M. A.; Holmes, J. D. *ChemPhysChem* **2011**, *12*, 2995−3001.

(16) Yoshikawa, N.; Ishizuka, E.; Taniguchi, S. *Mater. Trans.* **2006**, *47*, 898−902.

(17) (a) Goethel, P. J.; Yang, R. T. *J. Catal.* **1986**, *101* (2), 342−351. (b) Goethel, P. J.; Yang, R. T. *J. Catal.* **1987**, *108* (2), 356−363. (c) Goethel, P. J.; Yang, R. T. *J. Catal.* **1989**, *119* (1), 201−214. (d) Mehedi, H.-a.; Arnault, J.-C.; Eon, D.; Hebert, C.; Carole, D.; Omnes, F.; Gheeraert, E. *Carbon* **2013**, *59*, 448−456.

(18) Vivas-Castro, J.; Rueda-Morales, G.; Ortega-Cervantez, G.; Moreno-Ruiz, L.; Ortega-Aviles, M.; Ortiz-Lopez, J. Synthesis of Carbon Nanostructures by Microwave Irradiation. In *Carbon Nanotubes - Synthesis, Characterization, Applications*; Yellampalli, S., Eds.; InTech: 2011.

(19) (a) Ramasse, Q. M.; Zan, R.; Bangert, U.; Boukhvalov, D. W.; Son, Y. W.; Novoselov, K. S. *ACS Nano* **2012**, *6*, 4063−4071. (b) Demidov, D. V.; Prosvirin, I. P.; Sorokin, A. M.; Bukhtiyarov, V. I. *Catal. Sci. Technol.* **2011**, *1*, 1432−1439.

(20) Gordeev, E. G.; Polynski, M. V.; Ananikov, V. P. *Phys. Chem. Chem. Phys.* **2013**, *15*, 18815−18821.

(21) (a) Dral, P. O.; Kivala, M.; Clark, T. *J. Org. Chem.* **2013**, *78*, 1894−1902. (b) Panigrahi, S.; Bhattacharya, A.; Banerjee, S.; Bhattacharyya, D. *J. Phys. Chem. C* **2012**, *116*, 4374−4379. (c) Wang, W.; Zhang, Y.; Wang, Y. B. *J. Chem. Phys.* **2014**, *140*, 094302.

(22) Selected examples: (a) Acik, M.; Chabal, Y. J. *Jpn. J. Appl. Phys.* **2011**, *50* (7), 070101. (b) Zhang, X.; Xin, J.; Ding, F. *Nanoscale* **2013**, *5* (7), 2556−2569. (c) Kim, K.; Coh, S.; Kisielowski, C.; Crommie, M. F.; Louie, S. G.; Cohen, M. L.; Zettl, A. *Nat. Commun.* **2013**, *4*, 2723. (d) He, K.; Lee, G. D.; Robertson, A. W.; Yoon, E.; Warner, J. H. *Nat. Commun.* **2014**, *5*, 3040. (e) Wagner, P.; Ivanovskaya, V. V.; Melle-Franco, M.; Humbert, B.; Adjizian, J.-J.; Briddon, P. R.; Ewels, C. P. *Phys. Rev. B* **2013**, *88* (9), 094106.

(23) Homma, Y. *Catalysts* **2014**, *4* (1), 38−48.

(24) Mattevi, C.; Kim, H.; Chhowalla, M. *J. Mater. Chem.* **2011**, *21* (10), 3324−3334.

(25) (a) Becke, A. D. *Phys. Rev. A* **1988**, *38*, 3098−3100. (b) Lee, C.; Yang, W.; Parr, R. G. *Phys. Rev. B* **1988**, *37*, 785−789. (c) Becke, A. D. *J. Chem. Phys.* **1993**, *98*, 5648−5652.

(26) (a) Zhao, Y.; Truhlar, D. G. *Theor. Chem. Acc.* **2008**, *120*, 215−241. (b) Zhao, Y.; Truhlar, D. G. *Acc. Chem. Res.* **2008**, *41*, 157−167.

(27) Zhao, Y.; Truhlar, D. G. *J. Chem. Phys.* **2006**, *125*, 194101.

(28) Chai, J.-D.; Head-Gordon, M. *Phys. Chem. Chem. Phys.* **2008**, *10*, 6615−6620.

(29) (a) Hehre, W. J.; Ditchfield, R.; Pople, J. A. *J. Chem. Phys.* **1972**, *56*, 2257−2261. (b) Hariharan, P. C.; Pople, J. A. *Theor. Chim. Acta* **1973**, *28*, 213−222.

(30) Frisch, M. J.; Trucks, G. W.; Schlegel, H. B.; Scuseria, G. E.; Robb, M. A.; Cheeseman, J. R.; Scalmani, G.; Barone, V.; Mennucci, B.; Petersson, G. A.; Nakatsuji, H.; Caricato, M.; Li, X.; Hratchian, H. P.; Izmaylov, A. F.; Bloino, J.; Zheng, G.; Sonnenberg, J. L.; Hada, M.; Ehara, M.; Toyota, K.; Fukuda, R.; Hasegawa, J.; Ishida, M.; Nakajima, T.; Honda, Y.; Kitao, O.; Nakai, H.; Vreven, T.; Montgomery, J. A., Jr.; Peralta, J. E.; Ogliaro, F.; Bearpark, M.; Heyd, J. J.; Brothers, E.; Kudin, K. N.; Staroverov, V. N.; Keith, T.; Kobayashi, R.; Normand, J.; Raghavachari, K.; Rendell, A.; Burant, J. C.; Iyengar, S. S.; Tomasi, J.; Cossi, M.; Rega, N.; Millam, J. M.; Klene, M.; Knox, J. E.; Cross, J. B.;

Bakken, V.; Adamo, C.; Jaramillo, J.; Gomperts, R.; Stratmann, R. E.; Yazyev, O.; Austin, A. J.; Cammi, R.; Pomelli, C.; Ochterski, J. W.; Martin, R. L.; Morokuma, K.; Zakrzewski, V. G.; Voth, G. A.; Salvador, P.; Dannenberg, J. J.; Dapprich, S.; Daniels, A. D.; Farkas, O.; Foresman, J. B.; Ortiz, J. V.; Cioslowski, J.; Fox, D. J. *Gaussian 09*, Revision D.01; Gaussian, Inc.: Wallingford, CT, 2013.

(31) Stewart, J. J. P. *J. Mol. Model.* **2007**, *13*, 1173−1213.

(32) (a) Stewart, J. J. P. *MOPAC2012*, Ver. 13.296L; Stewart Computational Chemistry: Web: HTTP://OpenMOPAC.net (accessed Aug 30, 2014). (b) Maia, J. D. C.; Urquiza Carvalho, G. A.; Mangueira, C. P.; Santana, S. R.; Cabral, L. A. F.; Rocha, G. B. *J. Chem. Theory Comput.* **2012**, *8*, 3072−3081.

(33) Chuvilin, A.; Kaiser, U.; Bichoutskaia, E.; Besley, N. A.; Khlobystov, A. N. *Nat. Chem.* **2010**, *2*, 450−453.